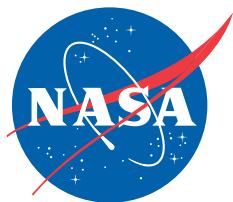NASA/TP–2007-213492

Zeta Pegasi: An SPB Variable Star

John H. Goebel
Ames Research Center, Moffett Field, California

January 2007

The NASA STI Program Office . . . in Profile

Since its founding, NASA has been dedicated to the advancement of aeronautics and space science. The NASA Scientific and Technical Information (STI) Program Office plays a key part in helping NASA maintain this important role.

The NASA STI Program Office is operated by Langley Research Center, the Lead Center for NASA's scientific and technical information. The NASA STI Program Office provides access to the NASA STI Database, the largest collection of aeronautical and space science STI in the world. The Program Office is also NASA's institutional mechanism for disseminating the results of its research and development activities. These results are published by NASA in the NASA STI Report Series, which includes the following report types:

- TECHNICAL PUBLICATION. Reports of completed research or a major significant phase of research that present the results of NASA programs and include extensive data or theoretical analysis. Includes compilations of significant scientific and technical data and information deemed to be of continuing reference value. NASA's counterpart of peer-reviewed formal professional papers but has less stringent limitations on manuscript length and extent of graphic presentations.

- TECHNICAL MEMORANDUM. Scientific and technical findings that are preliminary or of specialized interest, e.g., quick release reports, working papers, and bibliographies that contain minimal annotation. Does not contain extensive analysis.

- CONTRACTOR REPORT. Scientific and technical findings by NASA-sponsored contractors and grantees.

- CONFERENCE PUBLICATION. Collected papers from scientific and technical conferences, symposia, seminars, or other meetings sponsored or cosponsored by NASA.

- SPECIAL PUBLICATION. Scientific, technical, or historical information from NASA programs, projects, and missions, often concerned with subjects having substantial public interest.

- TECHNICAL TRANSLATION. English-language translations of foreign scientific and technical material pertinent to NASA's mission.

Specialized services that complement the STI Program Office's diverse offerings include creating custom thesauri, building customized databases, organizing and publishing research results . . . even providing videos.

For more information about the NASA STI Program Office, see the following:

- Access the NASA STI Program Home Page at *http://www.sti.nasa.gov*

- E-mail your question via the Internet to help@sti.nasa.gov

- Fax your question to the NASA Access Help Desk at (301) 621-0134

- Telephone the NASA Access Help Desk at (301) 621-0390

- Write to:
  NASA Access Help Desk
  NASA Center for AeroSpace Information
  7115 Standard Drive
  Hanover, MD 21076-1320
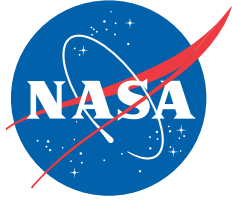
Zeta Pegasi: An SPB Variable Star

John H. Goebel
Ames Research Center, Moffett Field, California

National Aeronautics and
Space Administration

Ames Research Center
Moffett Field, California 94035-1000

ACKNOWLEDGMENTS

TABLE OF CONTENTS

LIST OF FIGURES

LIST OF TABLES

INTRODUCTION

During the course of the Gravity Probe B (GP-B) mission, the star Zeta Pegasi (ζ Peg) was observed for 27 hr. The opportunity to observe the star was the by-product of gyroscope torque calibrations at the end of the science mission. The scheduling of repeated observing periods was incompatible with the mission plan.

The European Space Agency's Hipparcos star-fixing satellite performed photometry of stars brighter than 8th magnitude. It observed 118,218 objects, some with a precision of 0.2 (6) mmag for a 5th (9th) m_V star (vanLeeuwen et al. 1997). For ζ Peg, the precision is no better than 2 mmag, and more frequently is considerably worse. The observations were consistent with constant brightness to that level of accuracy.

The Hubble Space Telescope (HST) fine guidance sensor capability for photometric precision is <500 ppm (500 μmag or 0.5 mmag) and at best 50 ppm (0.05 mmag) for stars in the brightness range 9th to 11th magnitude after averaging for a few hours (Zwintz et al. 2000).

The photometric precision level that we report is not unprecedented for a space-based observatory. What is new is that such precise observations have not been made of this bright star. ζ Peg is widely used as a spectrophotometric standard from ground-based observatories.

OBSERVATIONS

The photometer consists of multiple silicon diode detectors arranged in bicell pairs and full redundancy for the purpose of guide star tracking. That is, eight detectors are amplified independently, with each quartet redundant. Each bicell pair measures the light from half the field of view (FOV), which is divided by a knife-edge or rooftop mirrors arranged orthogonally. This quadrant arrangement provides signals to the guidance system sensitive to deviations in spacecraft body fixed X and Y coordinates. The detector modules are described in Demroff et al. (1998). A diagram of the telescope is shown in figure 1. Note the Image Divider Assembly (IDA) and the pair of Detector Package Assemblies (DPA), one for the X-axis and one for the Y-axis. Each DPA has a pair of bicells, along with a beamsplitter that creates redundant channels.

The optical channels created by the IDA are not identical, leading to the need for numerical weighting factors for the conversion from individual detector electron current to photon rate. Imbalances in each optical channel contribute to an imbalance in bicell signals. For pointing purposes the imbalances are accounted for. They have no substantial effect on the resulting photometry presented here, which results from totalizing the four bicells without weighting factors. To first approximation, the deviation signals in a bicell pair cancel out upon summation of the pair.

An observation consists of the mean value of all points during a given guide star valid (GSV) period and the statistical accuracy (standard deviation normalized by the square root of the number of samples) with which that mean value is reported. Hence one observation is made every orbit. During the course of the science phase of the mission, about 6000 observations of guide stars were performed. A day has 15 orbits.

Any chosen guide star is observed in staring mode as continuously as possible. A GSV period is typically 55 min of a 97-min orbital period. Guide star invalid (GSiV) is the remaining time when the telescope is pointed at the Earth. Three to five orbits are usually affected by the South Atlantic Anomaly (SAA) and require data filtering or censoring.

Silicon diode detector data are sampled at a 10 Hz rate. All eight detectors are sampled simultaneously and recorded to a spacecraft computer and then transmitted during a ground pass. Occasionally, on average less than 0.7% of the time outside the SAA, a sample is corrupted by a recognizeable proton hit. Data grading routines remove the corrupted sample, replacing it with an average of the value for adjacent sample times. SAA time periods are regularly rejected entirely because during quiet solar epochs the proton hit rate approaches 100% of the samples. Conscious of the potential for a false 24-hr signal at some low level, we have examined data from the other stars for evidence of a 24-hr period and found nothing down to the noise level.

The GP-B quadrant tracking system is similar, conceptually, to the HST fine guidance system (Kallinger et al. 2005), having a four times slower readout rate. HST data are corrected for proton hits in the SAA by modeling the SAA flux and then subtracting from the observations. The slower readout rate for GP-B does not permit an accurate use of the HST SAA correction model.

An intermediate timescale average of the data stream is created by boxcar averaging 2-sec intervals in a database compaction procedure named preprocessing. Subsequently all eight detectors are summed in time register, and it is these data from which the photometry results are constructed.

Other instrumental and environmental effects on the data quality are handled by filtering out those time periods corresponding to low-quality data. For photometry purposes, roughly 37% of the detector readings are compromised in one fashion or another and discarded. Most notably, the first 15 min of a GSV can be corrupted by thermal instabilities of the DPA, and the last 5 min by atmospheric emission irregularities.

Detector data are routed to an onboard multiplexer and analog-to-digital converter, the design of which produces an electronic zero-shift that can be removed by observing dark sky. At various times during the mission dark observations were made. They were not regularly performed because the act of intentionally moving the pointing direction off the guide star was forbidden by science operation procedures. This restriction was for good reason. Moving the pointing position would introduce an unknown torque on the primary science gyroscopes. Fortunately for photometry purposes, there were occasional unintentional losses of guide star incidents that also produced dark sky observational periods. Furthermore, a few periods were available from the initial orbital checkout (IOC) and the final science gyroscope calibration (SGC) periods. Zero shifts were consistent during these periods.

During the science phase of the mission, only one star, IM Peg, was observed. During the IOC and guide star calibration (GSC) phases, a few other stars were observed. These other stars are the topic of this discussion. One was the photometric comparison star HD 216635 ($m_V = 6.612$, $B-V = 0.992$, K0). Observations of this star have been used to place the GP-B photometry on a scale of magnitudes. Stellar characteristics are in table 1. Data are from the SIMBAD database.

In the MK photometric system (Allen & Cox 2000), the color correction from HD 216635 with spectral type K0V is $V-R = +0.64$. Here the effective wavelength is approximately $\lambda_{GP-B} \sim R$. This color correction sets the accuracy limit of any quoted magnitude for GP-B to about 10 mmag. Thus we define the GP-B standard HD 216635 to have magnitude 6.612-0.64 = 5.9720000000000 (zeros added to emphasize definition). We recognize that a scale factor in the GP-B magnitude system remains unevaluated.

TABLE 1. STARS OBSERVED DURING THE GP-B MISSION ORDERED BY RA

Name	Spectral type	m_V (mag)
ζ Peg	B8V	3.402
IM Peg	K1.5II-IIIe	5.892
HD 216635	K0	6.612
HR Peg	S	6.471
α Peg	B9III	2.490

There were 85 observations of HD 216635 during the calibration portion of the mission. The observations are displayed in figure 2 and summarized in table 2. Note that the errors of the set of all observations, standard deviation ($\Delta m_{GP\text{-}B}$), exceed those of any single observation by an order of magnitude. It has not yet been determined if there is any credible reason to doubt the brightness constancy of this star. There is no obvious pattern to the scatter in measured values; there is no significant periodicity in the observation in the range of periods 0.2 to 5 days; see figure 3.

TABLE 2. COMPARISON OF OBSERVATIONS

Star	Mean of all observations ($m_{GP\text{-}B}$)	All observations errors ($\pm\Delta m_{GP\text{-}B}$)	Single observation errors ($\pm\Delta m_{GP\text{-}B}$)	Units
α Peg	2.12051553±0.010	0.0000466245	0.00004647150	mag
ζ Peg	3.04937900±0.010	0.0002762995	0.00005243297	mag
HD 216635	5.97200000±0.010	0.0053165300	0.00042985000	mag

In table 2, note that $\pm\Delta m_{GP\text{-}B}$ is more than 10 times larger for the standard star than for ζ Peg. The noise sources present while making any measurement are the same; what is different is the brightness of the two stars. Electronic amplifier noise is significant for HD 216635 relative to the star brightness; i.e., the signal-to-noise ratio (S/N) is low. For ζ Peg the S/N is higher. The same S/N issue is apparent in the results for α Peg, which is even brighter. There the observational results are shown in table 2.

For α Peg, the standard deviation ($\Delta m_{GP\text{-}B}$) of 6 observations is 46.62 μmag, while that of all 2-sec data points (1650) comprising any one observation is 46.47 μmag. So for a very bright star, there is no evidence of variability or gross instability of the photometer on the timescale of 12 hours (see fig. 4).

For ζ Peg, B8V, m_V = 3.4 (Hoffleit et al. 1982), 18 observations were made; see table 2. Observations of ζ Peg also show elevated errors of the set of all observations compared with those of individual observations. Unlike HD 216635, ζ Peg displays a distinct pattern in figure 5 that is apparent even in the raw data of figure 6.

The value of $m_{GP\text{-}B}$ is quoted with a confidence interval that reflects the statistics of the measurement procedure. The precise value for m_{GPB} is not central to the observation of variability.

From this comparison, it is seen that the errors (precision) of single or multiple observations decrease with increasing stellar brightness. There is a noise floor to the measurements setting the detectability limit for a faint star. The limit is 8.4 mag fainter than HD 216635, or the equivalent of 14.4 $m_{GP\text{-}B}$ for a single observation.

For HD 216635, errors of the set of all observations are elevated above the errors of any single observation, implying a source of low-frequency instrumental drift, i.e., $f^{-\alpha}$ noise. It does not greatly impair the instrumental performance, being a penalty of only 26%.

DISCUSSION

The observations of ζ Peg were modeled with a single sinusoidal oscillation. Derived parameters, e.g., brightness m_{GP-B}, sinusoidal amplitude A_0, period T, and Julian Date of phase zero $JD(\Phi_0)$, are listed in table 3. Also listed are the derived 95% confidence intervals from the nonlinear least-squares fit. Additional harmonics of this period were evaluated, and found to be unjustified at the level of confidence demanded by the observations.

TABLE 3. DERIVED PARAMETERS AND FORMAL ERRORS FOR ζ PEG

Parameter	Estimate ± accuracy	95% precision confidence interval	Units
m_{GP-B}	3.0483588	0.0000451	mag
A_0	0.0004882	0.0000066	mag
T	22.952	0.804	hr
$JD(\Phi_0)$	2453610.76987	0.0335	JD

A comparison of the derived parameters with the observations is shown in figure 7. The Julian date is not corrected for heliocentricity, which introduces a correction of no more than 5.775×10^{-3} day (Budding 1993).

ζ Peg is a double star system listed in the Washington Double Star Catalogue (Hartkopf, Mason, & Worley 2001; Hartkopf, McAlister, & Mason 2001; Mason et al. 2001; and Worley, Mason, & Wycoff 2001), the secondary or companion star being 8.2 mag fainter than the primary at the relative position (68 arcsec, 139°) (Worley & Douglass 1997). Nominally, the guide telescope has an FOV = 60 arcsec radius. This puts the secondary about 2 diffraction disks outside the nominal FOV, a bit too close to escape entanglement. From laboratory testing, the angular response at the FOVs perimeter declines slowly, starting its fall at 40 arcsec and decreasing somewhat linearly out to 75 arcsec. The perimeter is less well focused than the center, where the decline occurs in the span of 10 arcsec (see fig. 7). Consequently a fraction of light from the companion is seen in the GP-B observations, estimated to be as much as 30% of the total light from the companion.

Evaluation of the possible confusion imposed by the companion hinges on two parameters. First is the component of detector signal at the spacecraft roll rate. This is the primary scientific sampling frequency, so the pointing system (Automatic Tracking and Control, ATC) was designed to eliminate or at worst minimize any telescope signal at that frequency (12.9 mHz). Because of the imbalances in the optical channels, modulation at the roll frequency could be expected to be on the order of 50% of the companion star intensity. Unfortunately, technical difficulties prevented the complete realization of the requirement that no pointing component at the roll frequency creep into the pointing and control system. No accurate measurement of the secondary star at roll frequency is possible, as will now be discussed.

The ATC rate gyroscope, distinct from the science gyroscope, introduced a significant roll-rate signal to the ATC subsystem. The undesirable side effect was the introduction of a roll component into the detector signal of the guide star telescope. With the quadrant division of the FOV, one would expect to find a square wave modulation induced by the star crossing over the knife-edge and at the period of roll in the totalized signal. A 10-dB notch filter was introduced into the rate gyroscope signal line intended to block this false roll-rate component from corrupting the guide star signals. Harmonics of roll frequency resulted. For the science gyroscopes, this compromise was an acceptable one. In spite of these efforts to remove the roll frequency from the guide star telescope signal, there is still an observable residual roll-rate signal of sufficient magnitude to overwhelm any possible contribution by the companion star to the observations of ζ Peg at roll frequency.

Second is the stability in the pointing position from observation to observation. The guide star tracking position centering bias and noise of the spacecraft at the observation epoch of ζ Peg was as good as at any other time during the mission. For a typical observation, the mean pointing position, or centering bias from numerical zero, relative to the FOV center is shown in table 4. A statistical summary of the set of all observations of ζ Peg is given in table 5.

TABLE 4. TYPICAL GUIDE STAR CENTERING IN THE GP-B FOV FOR AN OBSERVATION OF ζ PEG

Parameter	Centering bias from zero	1σ confidence interval	Units
A-X	0.03135	0.086340	arcsec
A-Y	0.18677	0.080896	arcsec
B-X	0.10960	0.088649	arcsec
B-Y	0.182872	0.079467	arcsec

TABLE 5. CENTERING BIAS STATISTICS FOR ALL OBSERVATIONS OF ζ PEG

Parameter	Mean zero bias (NP) all orbits	1σ in bias (NP) all orbits	Mean zero bias all orbits	1σ in bias all orbits	Units
A-X	0.0103073	0.000401243	0.032589	0.00126054	arcsec
A-Y	0.0592183	0.000195411	0.186040	0.00061390	arcsec
B-X	0.0353156	0.000419219	0.110947	0.00131702	arcsec
B-Y	0.0579325	0.000194140	0.182000	0.00060991	arcsec

JD 24530606.3421348 is average time of all ζ Peg observations.

For there to be an instrumental origin to the ζ Peg variation in brightness, the pointing position observations would have to demonstrate a monotonic angular time series deviation about the center, perhaps circular; i.e., in proper sequence one orbit to another, with the required period and

amplitude. The time series of centering bias for the observations of ζ Peg is shown in figure 8. The excursions of the bias show no significant circular pattern in excess of 1 marcsec; see figure 9.

Furthermore, the differential pointing design cancels the photocurrent from a pair of detectors, within the limits of design and manufacture. Thus a companion star that is in the FOV and displaced significantly beyond the diffraction disk of the main guide star will contribute a signal that is small compared with its relative brightness. A star well beyond the diffraction disk of the primary star will produce a decreasingly small signal until it nears the perimeter of the FOV. In the case of ζ Peg, the star is at the perimeter of the FOV; see figure 10. The rate at which the companion signal falls with angle at the edge of the FOV is about 5 times less rapid at the knife-edge in the FOVs center where the main guide star image division takes place. At the edge, the decline is equivalent to 200 marcsec/unit normalized pointing compared with about 800 marcsec/unit normalized pointing at the center. This verbal description of the normalized pointing function can be visualized as the derivative of the transmission curves in figure 11.

For any one of the detectors, typical signal modulation from displacement at the FOV edge is, in a relative sense, 100%/30 arcsec, where 30 arcsec is the angular region of declining response, and falls off approximately linearly. So %mod/marcsec = (1 marcsec/100% × 30 arcsec) = 3.3×10^{-3} %/marcsec modulation of secondary star signal in that edge region. The companion brightness is 3.4 + 8.2 = 11.6 m_V (Worley & Douglass 1997). For a perfectly balanced main guide star tracking signal, the secondary modulation would be $-2.5 \times \log_{10}(3.3 \times 10^{-3}) = 6.2$ m_V/marcsec equivalent. Relative to the main guide star this is a modulation of (3.4 + 6.2) or 9.6 m_V, which compares with the stellar brightness difference of 8.2 m_V. In contrast, if the companion were intrinsically the source of variation, its amplitude would be 8.2 – 9.6 = –0.6 m_V and needs to have a period of 22.9 hr. This compares with the observed total emission modulation of 488 μm_V at 3.6 m_V, which is equivalent to a secondary of 3.6 + 8.3 = 11.9 m_V. So, at the marcsec pointing stability level, the secondary is bright enough to account for the modulated signal of ζ Peg. However, the pointing is somewhat more stable than 1 marcsec, being at the 0.1-marcsec level. This makes the stellar equivalent variation that of a (11.6 + 2.5 =)14.1 m_V secondary. So more information needs to be collected on the secondary. Later on, this will be seen to transfer the problem of intrinsic primary variation, which can easily be accounted for by the primary to that of the secondary, which is more problematic.

Occasionally during science mission operations, optical events produced spurious signals in all the detectors simultaneously (see fig. 12). These signals lasted for no more than a fraction of a GSV period. The intensity of these signals varied widely and may be attributed to the sudden appearance and dissipation of clouds of gas and particles at orbital altitudes. There was no discernable effect on the spacecraft pointing at these times. None of these events occurred during the observations of ζ Peg.

On August 22, 2005, at 00h 00m 00s Universal Time (UT), the time when ζ Peg was being observed, the sun was at right ascension (RA) 10h 04m 33.4s; declination (DEC) 11° 49′ 13.7″ (http://aa.usno.navy.mil/data/docs/geocentric.html). So the sun was directly behind the spacecraft. The moon was at 00h 04m 09.4s –00° 53′ 42″ in waxing gibbous phase of 0.91, and was 30.5° to the port side of the spacecraft. The rejection pattern of the telescope and sunshade put the moon well outside the limits of detectability. Observations of other fainter guide stars preceding and

following those of ζ Peg showed no indications of scattered Lunar light. Of course during GSV, the Earth is also behind the spacecraft. Hence there are no scattered light issues during the observations of ζ Peg.

A 24-hr period induced by the SAA proton activity in the telescope detectors is a concern. The best-fit period for ζ Peg is significantly under 24 hr. If the proton activity in the detectors were the origin, then one would expect that the detector currents would be elevated slightly at times near the SAA passage time. In fact, the opposite is the case; the current is depressed at this time. A step to lower currents for the 3 or 4 orbits of SAA and the return therefrom would be anticipated, and a following phase relationship of the detector currents to the SAA would imply a causal relationship. No such correlation exists. See figure 5.

Contributions to the detector currents during passage through the polar regions are expected to exhibit behavior similar to the SAA passage. The proton rate during those intervals is sufficiently low to exclude them from consideration.

Hence we are led to conclude that the origin of the micromagnitude scale variability that is seen in the data for ζ Peg is intrinsic to the star. The 488-mmag amplitude is within the measurement capabilities of the WIRE spacecraft guidance sensor (Buzasi et al. 2005).

Variability Classification

One possible source of variability is starspots that can produce a sinusoidal oscillation in the brightness (Sterken & Jaschek 1996) if the size, position, and darkness (brightness) parameters are correctly chosen. Based on current thinking, B-type stars are not suspected to harbor starspots. This possibility cannot be eliminated by the present observations alone. If we are observing the fundamental, a cooler region, i.e., spot covering a substantial portion of the surface of the star, would be required for a sinusoidal light curve. A rotational period of one day seems a bit quick, even for a B star.

First we compare the observations of another B with somewhat similar characteristics that were studied by Zwintz, et al. (2000) (see the following quote (italic) and tables 1 and 2).[*]

"VGS 15, GS0739300128: There are two data sets observed in 1992 and 1993, respectively, where the second set has a rather short (~2 hours) time base. A frequency of 1.05551 c/d fits the data from both years well, but Fig. 4 shows only the observations from 1992. A δ Sct light curve would be consistent with the TYCHO color and Strömgren photometry (late A), but not with B8 given in the SIMBAD archive."

TABLE 1. PARAMETERS FOR 20 VARIABLE GUIDE STARS (VGS) DISCUSSED IN THIS PAPER BASED ON AN AUTOMATIC ANALYSIS AND CLASSIFICATION*

VGS	GSC	JD$_{start}$	mag(V)	FGS	n_{dat}	$f_{max\,amp}$	noise	A_{max}	t_{base}	Cl
#	#	2447892+	(GSC)	#		(mHz)	(ppm)	(ppm)	(h)	
15	0739300128	955.0155	9.49	1	283177	0.0128	286.0	26431.53	24.48	t2
		1366.2859		1	11984	0.0893	1001.1	5957.05	1.94	o4

* VGS number; Guide Star Catalog number (GSC); time at start of observations in Julian Date (JDstart); magnitude given in the Guide Star Catalog (mag(V)); Fine Guidance Sensor used for a given data set (FGS); number of measurements for each data set ($n$dat); frequency at maximum amplitude ($f$max amp) in mHz; noise level in ppm; maximum amplitude (Amax) in ppm; time base ($t$base) in hours; classification (Cl) due to criteria described in Sect. 2. (Reprinted by permission of the publisher, Astronomy & Astrophysics (Dec. 2006).)

TABLE 2. RIGHT ASCENSION (RA) AND DECLINATION (DEC) FOR EPOCH 2000 FROM THE GUIDE STAR CATALOG (GSC)*

VGS	GSC	RA	DEC	Name	V	$B-V$	HIP	Sp	V_{simbad}	comment
		hh:mm:ss	°:′:″		TYCHO			SIMBAD		
15	0739300128	18:23:29	−30:15:30		9.8	0.192	HD168922	B8IV	9.81	δ Sct

* name; spectral type (Sp); V and $B-V$ from tycho catalog; number in the hipparcos catalog (HIP); spectral types (sometimes not consistent with $B-V$!) from the tycho catalog; merged Vsimbad from the simbad data base; preliminary identification of variability type (comment). (Reprinted by permission of the publisher, Astronomy & Astrophysics (Dec. 2006).)

The common definition of the δ Scuti variables is found at
http://cdsweb.u-strasbg.fr/afoev/var/edsct.htx
 (Centre de Données Astronomiques de Strasbourg 2006)

"Variables of the Delta Scuti type. These are pulsating variables of spectral types A0-F5 III-V displaying light amplitudes from 0.003 to 0.9 mag in V (usually several hundredths of a magnitude) and periods from 0.01 to 0.2 days. The shapes of the light curves, periods, and amplitudes usually vary greatly. Radial as well as nonradial pulsations are observed. The variability of some members of this type appears sporadically and sometimes completely ceases, this being a consequence of strong amplitude modulation with the lower value of the amplitude not exceeding 0.001 mag in some cases. The maximum of the surface layer expansion does not lag behind the maximum light for more than 0.1 periods. DSCT stars are representatives of the galactic disk (flat component) and are phenomenologically close to the SX Phe variables."

Although the δ Sct variables have similar variational amplitudes, their periods are only 1/10th that of ζ Peg. That places ζ Peg outside the range defined for the class, as well as outside the spectral class recognized for δ Sct variables.

The Slowly Pulsating B-Stars (SPB) (Waelkens 1991) have periods between about 1 and 3 days ranging over type classes (B3–B8), and are, therefore, more appropriate to ζ Peg. Typically they are multiperiodic and have low rotational velocities, $v\,sin(i) \sim 20$ km/sec unlike ζ Peg. The existence of another variable class characterized by similar spectral class and variability period leads to the

9

conclusion that ζ Peg is an example of a micromagnitude slowly pulsating B-type variable. Zwintz's comment that VGS 15 is like a δ Sct variable but with a B-type spectrum is taken to imply unfamiliarity with the general body of SPB research. The SPB class of variables is also distinct from the β Cep variables, which are nonradial pulsators of early B spectral class; i.e., O8 to B5 (Smith 1977).

At 191 km/sec, ζ Peg is a fast rotator (*v sin(i)* > 100 km/sec (Townsend 2003), an order of magnitude faster than standard SPB slow rotators (North & Paltani 1994). The brightness amplitude is much smaller than for slowly rotating SPB stars, so the anticorrelation suggests SPB behavior paralleling the behavior of δ Sct variables. The faster the rotation, the lower the brightness amplitude. Townsend stated "*that g-modes are excited, but that equatorial confinement by the Coriolis force may push their photometric signatures below typical observation detection limits*." Here we present observations consistent with that hypothesis. Currently cataloged SPB stars seem to be slow rotators (Waelkens 1991). It is our opinion that this is the result of observational bias.

Hypothetically, within the class of B-type stars there may be a positive correlation of g-mode amplitude with the stellar rotational velocity, the measure of angular momentum. This suggestion raises the question of whether for any evolving B star, g-mode oscillations coupled with Coriolis force-induced material transport can produce enough frictional dissipation to act as a braking mechanism on stellar rotation. One would expect the rotation rate to decrease as evolution progresses, as the star swells, and the amplitude of oscillation to increase. Analysis of this problem is beyond the scope of this report.

In the Herzsprung-Russell diagram shown in figure 13, ζ Peg lies just above the Hyades Cluster ZAMS line, indicating a slight degree of evolution off the main sequence. Also shown in the figure are the other stars that were observed by GP-B. The observed low-amplitude g-mode oscillation is consistent with the current understanding of stellar evolution and observations of other SPB stars. The B-V color implies an age of about 2.1×10^9 yr (fig. 14). Figure 15 locates the SPB variables in the HR diagram relative to other variable classes. With this in mind, it is appropriate to quote (Kurtz 2006):

"*There are three places in the Figure 11 pulsational HR diagram* (see fig. 15)*, where there are p-mode and g-mode pulsators of similar structure: for the β Cep (p-mode) and Slowly Pulsating B (SPB g-mode) stars on the upper main sequence; for the δ Sct (p-mode) and γ Dor (g-mode) stars of the middle main sequence; and for the EC 14026 sub-dwarf B variables (p-mode) and the PG 1716+426 stars (g-mode). Stars pulsating in both p-modes and g-modes promise particularly rich asteroseismic views of their interiors.*"

The topic of p-modes is reviewed by Christensen-Dalsgaard (2002) in application to the sun, under the term helioseismology. It has become an invaluable tool in the understanding of the neutrino problem. The acoustic oscillations measure properties of the solar interior, for which there is no other available tool.

Here we examine the potential for discovering p-mode oscillations (Kurtz 2006) in the observations of ζ Peg. In figure 16 the frequencies of acoustic p-modes are graphed for their degree, *l*, and order, *n*, along with the g-modes of a solar model. The graph is instructive as a relational tool for the

10

various modes and their mathematical parameters. Unless the amplitudes are extremely large, then because of the science gyroscopic observational frequency choice of 12.9 mHz (77.5 sec), there is considerable confusion with instrumental effects in the minute period range. The harmonics of roll and the dither frequencies further confuse the spectrum considerably.

Spectra of a single orbit for each of α Peg and ζ Peg display essentially white noise at frequencies above the dither frequencies, 29 and 34.5 mHz, and the 1st, 2nd, and 3rd harmonics of roll (12.8, 25.8, and 39.7 mHz). (See figure 17.) The 10-Hz Nyquist sampling limit accounts for the spectral rolloff between 1 and 5 Hz. Upon summation of all detectors, imperfect cancellation at these distinct frequencies leaves a residual at the strongest of discrete frequencies that are seen in the individual detector spectra. At frequencies between roll, 12.8 mHz, and the lowest frequency sampled, 600 μHz (see figure 18), the spectra of both stars are indistinguishable within a possible *1/f* rise in low-frequency noise. In this low-frequency range, any p-mode signals are at or below the instrumentation noise level. So we cannot discern any indication of acoustic p-modes in ζ Peg. Spectral resolution below 10 mHz is too coarse to obtain accurate frequency measurements there. We cannot say p-modes are present or absent near the noise level.

Because it is imprudent to attempt recovery of possible g-modes in the GP-B photometry, we will have to wait for the arrival of satellite observatories specifically designed for asteroseismology.

CONCLUSION

Based on photometric observations of ζ Peg from the GP-B guide star telescope, we find that the star is an SPB variable with a period of 22.952 hours (1.04566 c/d) and amplitude of 0.0004882 m_{GP-B}. This period is identified as a g-mode oscillation. No conclusive periods can be associated with p-mode oscillations in the 0.6- to 10-mHz region of the asteroseismological spectrum. Future precision photometry is necessary to confirm the resulting classification. It seems likely that micromagnitude photometry will produce a great many variable stellar classifications and a more complete understanding of the precise evolutionary status of otherwise mundane stars. With future space missions, substantial advances can be anticipated.

REFERENCES

Allen, C. W.: Allen's astrophysical quantities. Ed. A. N. Cox, New York, AIP Press:Springer, 2000.

Budding, E.: An Introduction to astronomical photometry. Cambridge, New York: Cambridge University Press, 1993.

Buzasi, D. L.; Bruntt, H.; Bedding, T. R.; et al.: Altair: The brightest delta Scuti star. Astrophysical J., vol. 619, no. 2, Feb. 2005, pp. 1072–1076.

Centre de Données Astronomiques de Strasbourg, C.: SIMBAD Astronomical Database. Centre de Données Astronomiques de Strasbourg, 2006.

Christensen-Dalsgaard, J.: Helioseismology. Reviews of Modern Physics, vol. 74, no. 4, Oct. 2002, pp. 1073–1129.

Demroff, H. P.; Babu, S.; Bye, M. R.; et al.: The telescope readout electronics for the Gravity Probe B satellite. J. De Physique IV, vol. 8, no. 3, June 1998, pp. 175–179.

Hartkopf, W. I.; Mason, B. D.; and Worley, C. E.: The 2001 US Naval Observatory Double Star CD-ROM. II. The Fifth Catalog of Orbits of Visual Binary Stars. Astronomical J., vol. 122, no. 6, 2001, pp. 3472–3479.

Hartkopf, W. I.; McAlister, H. A.; and Mason, B. D.: The 2001 US Naval Observatory Double Star CD-ROM. III. The Third Catalog of Interferometric Measurements of Binary Stars. Astronomical J., vol. 122, no. 6, Dec. 2001, pp. 3480–3481.

Hoffleit, D.; and Jaschek, C.: The bright star catalogue. New Haven, Conn.: Yale University Observatory, 1982.

Kallinger, T.; Zwintz, K.; Pamyatnykh, A. A.; et al.: Pulsation of the K2.5 giant star GSC 09137-03505? Astronomy & Astrophysics, vol. 433, no. 1, April 2005, pp. 267–273.

Kurtz, D. W.: Stellar pulsation: an overview. Communications in Asteroseismology, vol. 147, Jan. 2006, pp. 6–30.

Mason, B. D.; Wycoff, G. L.; Hartkopf, W. I.; et al.: The 2001 US Naval Observatory Double Star CD-ROM. I. The Washington Double Star Catalog. Astronomical J., vol. 122, no. 6, Dec. 2001, pp. 3466–3471.

North, P.; and Paltani, S.: Hd-37151—A New Slowly-Pulsating-B-Star. Pulsation, Rotation and Mass Loss in Early-Type Stars, vol. 162, 1994, pp. 41–42.

Smith, M. A.: Nonradial Pulsations in Early to Mid B Stars. Astrophysical J., vol. 215, no. 2, 1977, pp. 574–583.

Sterken, C.; and Jaschek, C.; Eds.: Light curves of variable stars: a pictorial atlas. Cambridge [England]; New York: Cambridge University Press, 1996.

Townsend, R. H. D.: A semi-analytical formula for the light variations due to low-frequency g modes in rotating stars. Monthly Notices of the Royal Astronomical Society, vol. 343, no. 1, July 2003, pp. 125–136.

vanLeeuwen, F.; Evans, D. W.; Grenon, W.; et al.: The Hipparcos mission: photometric data. Astronomy & Astrophysics, vol. 323, no. 1, 1997, pp. L61–L64.

Waelkens, C.: Slowly Pulsating B-Stars. Astronomy & Astrophysics, vol. 246, no. 2, June 1991, pp. 453–468.

Worley, C. E.; and Douglass, G. G.: The Washington Double Star Catalog (WDS, 1996.0). Astronomy & Astrophysics Supplement Series, vol. 125, no. 3, Nov. 1997, p. 523.

Worley, C. E.; Mason, B. D.; and Wycoff, G. L.: The 2001 US Naval Observatory Double Star CD-ROM. IV. The Photometric Magnitude Difference Catalog. Astronomical J., vol. 122, no. 6, Dec. 2001, pp. 3482–3484.

Zwintz, K.; Weiss, W. W.; Kusching, R.; et al.: Variable HST guide stars (I). Astronomy & Astrophysics Supplement Series, vol. 145, no. 3, Sept. 2000, pp. 481–490.
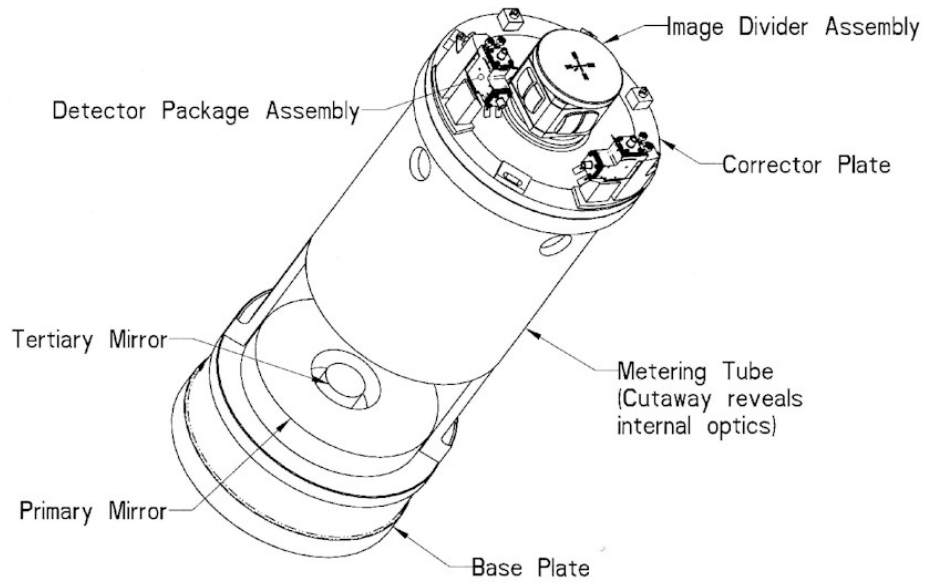
Figure 1. General view of GP-B telescope. Light enters from the top right.
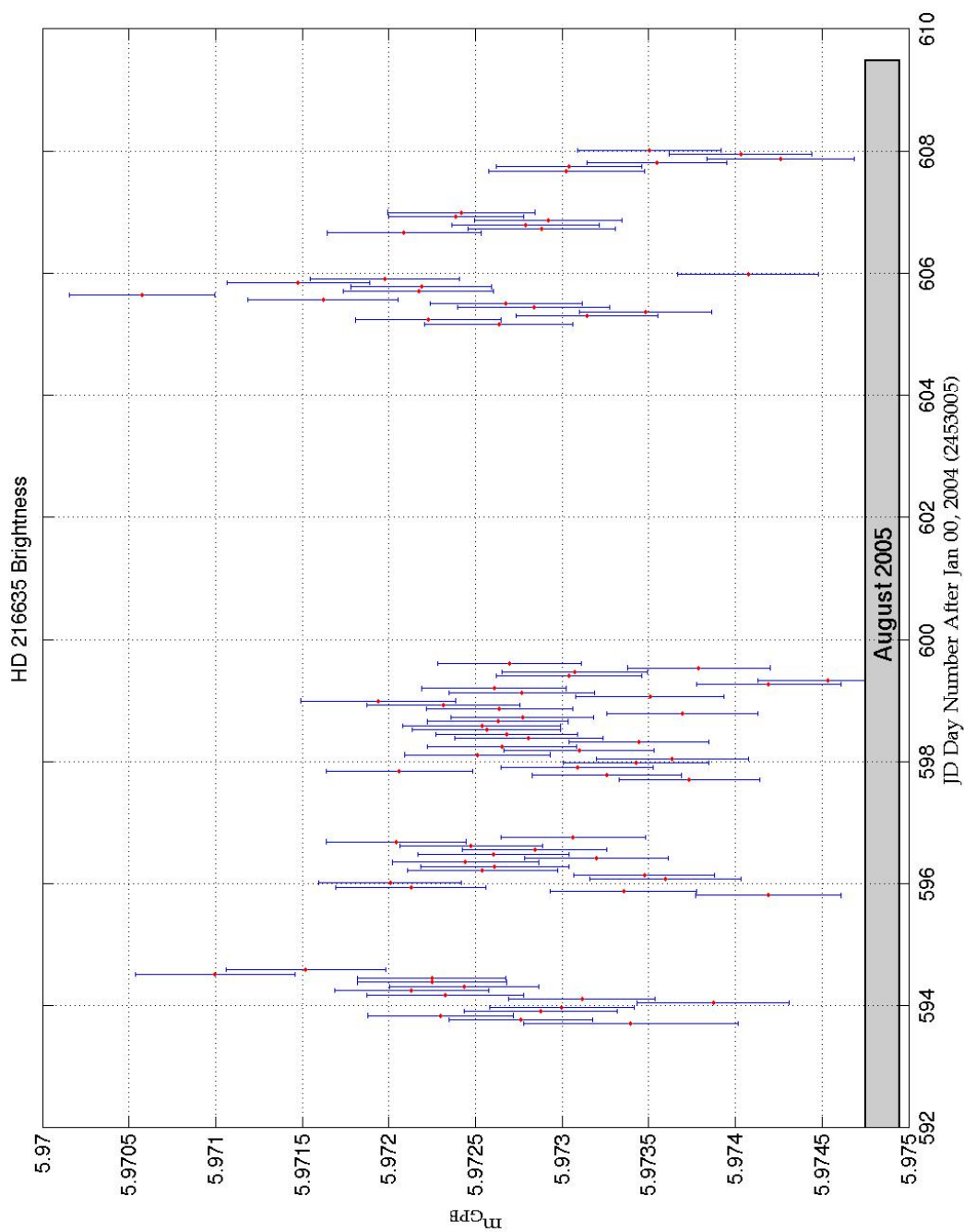
Figure 2. GP-B main guide telescope observations of HD 216635. Each datum is for a single orbit. Gaps in time result when observing something else.

16
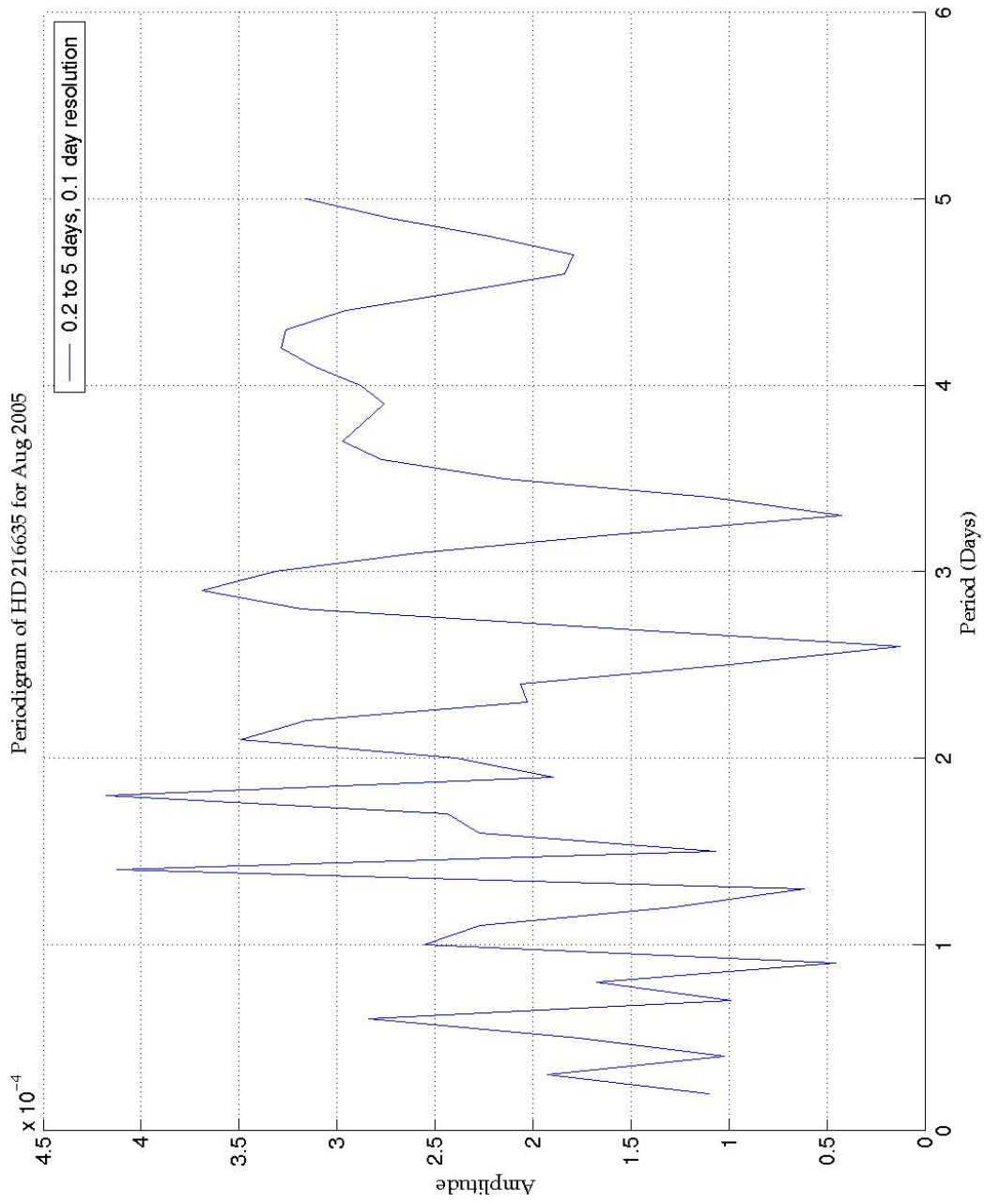
Figure 3. Periodigram of HD 216635 during the August 2005 time interval.
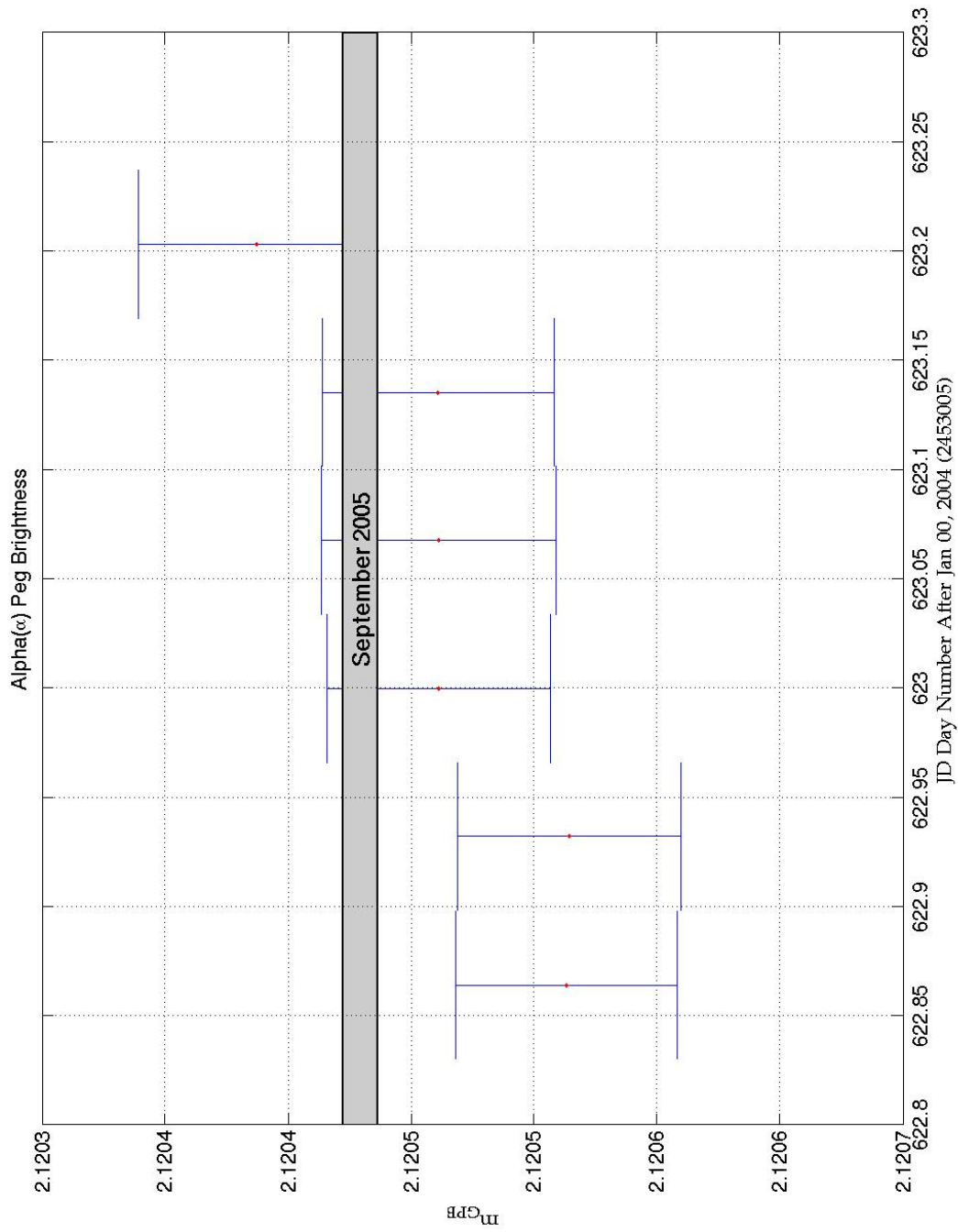
Figure 4. GP-B main guide telescope observations of α Peg.
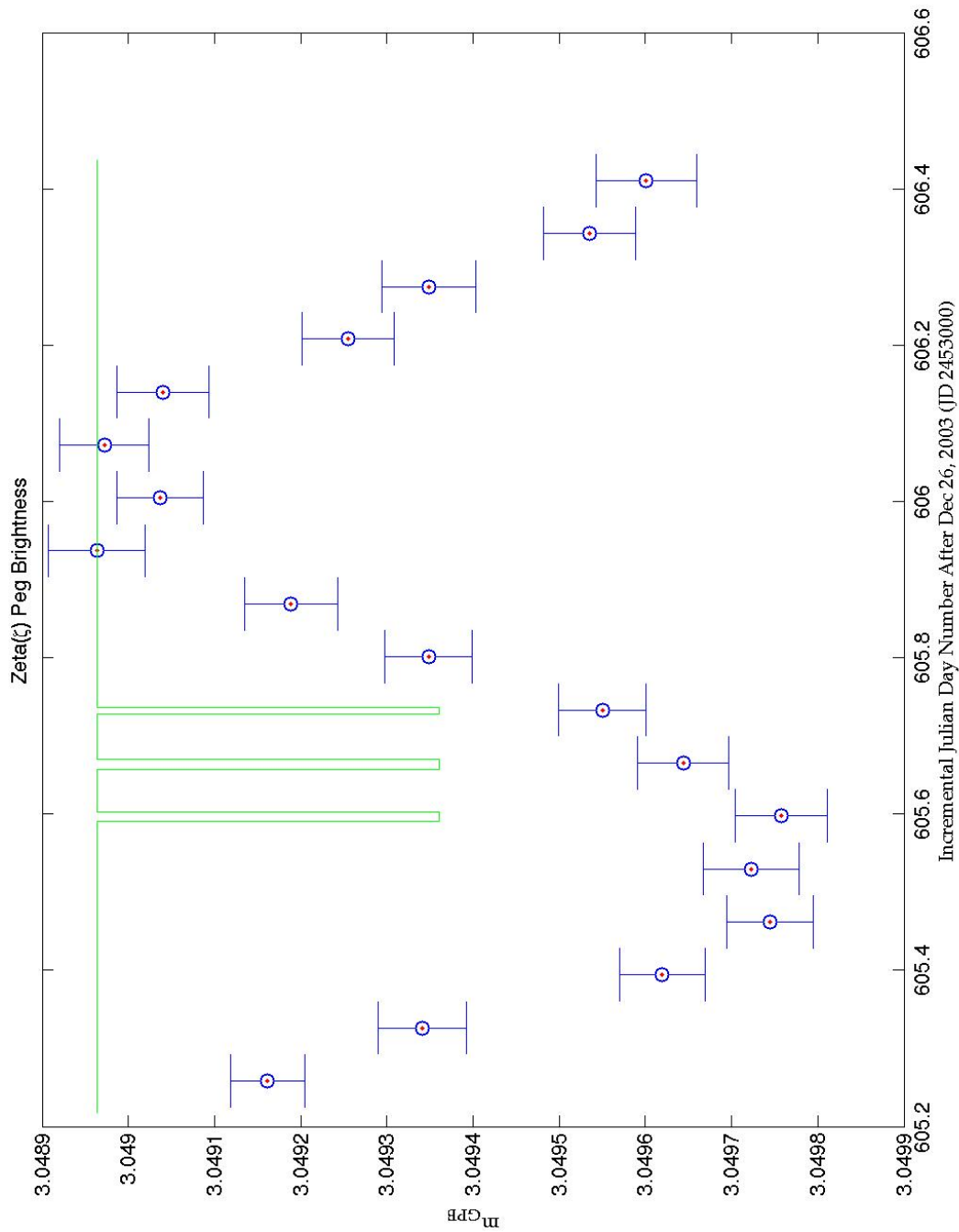
18

Figure 5. Observations of ζ Peg showing the positions of the SAA passes. The three vertical fingers locate the times of greatest SAA intensity.
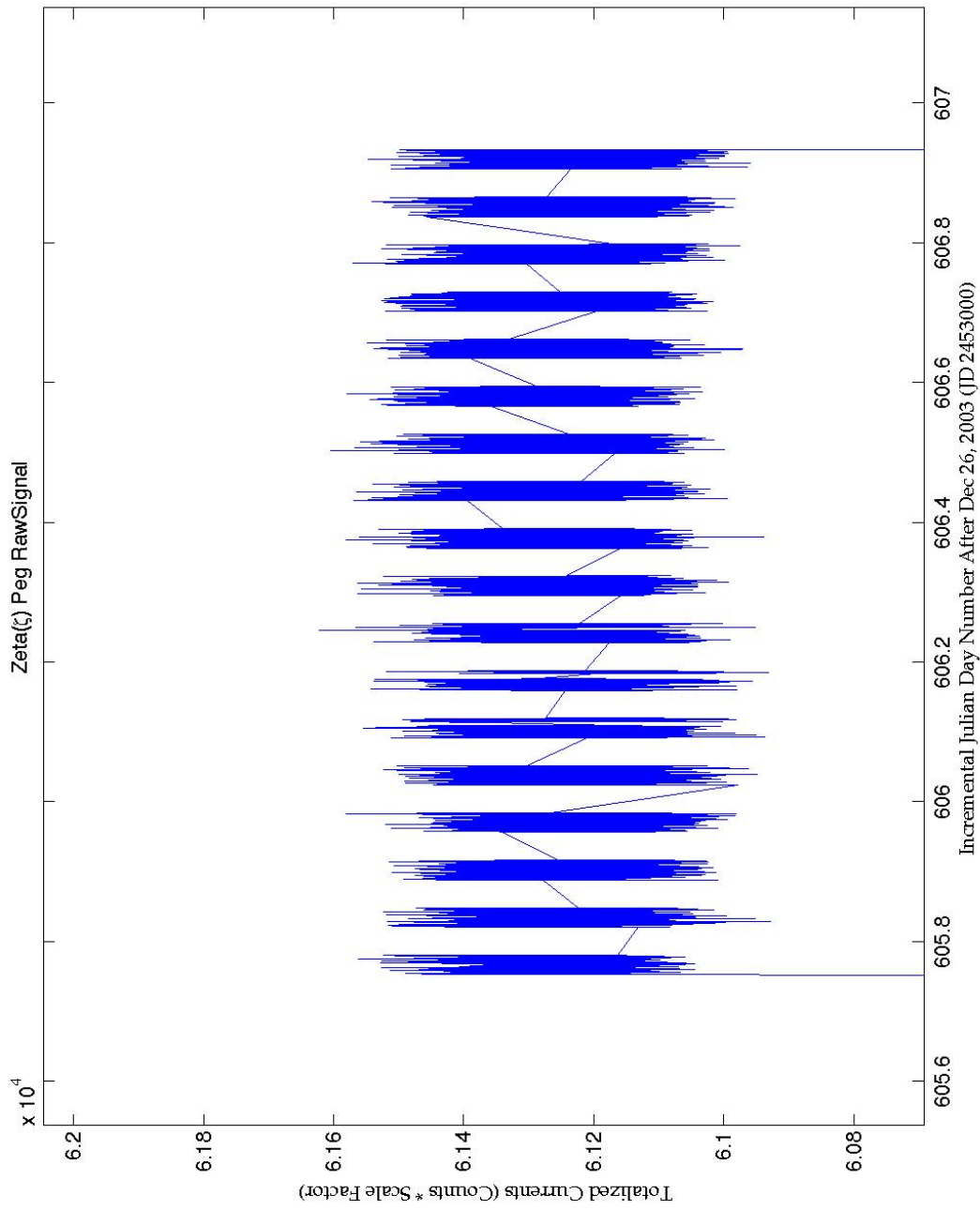
Figure 6. Raw counts for each 2-second datum showing the censoring during GSiV and SAA intervals.

20
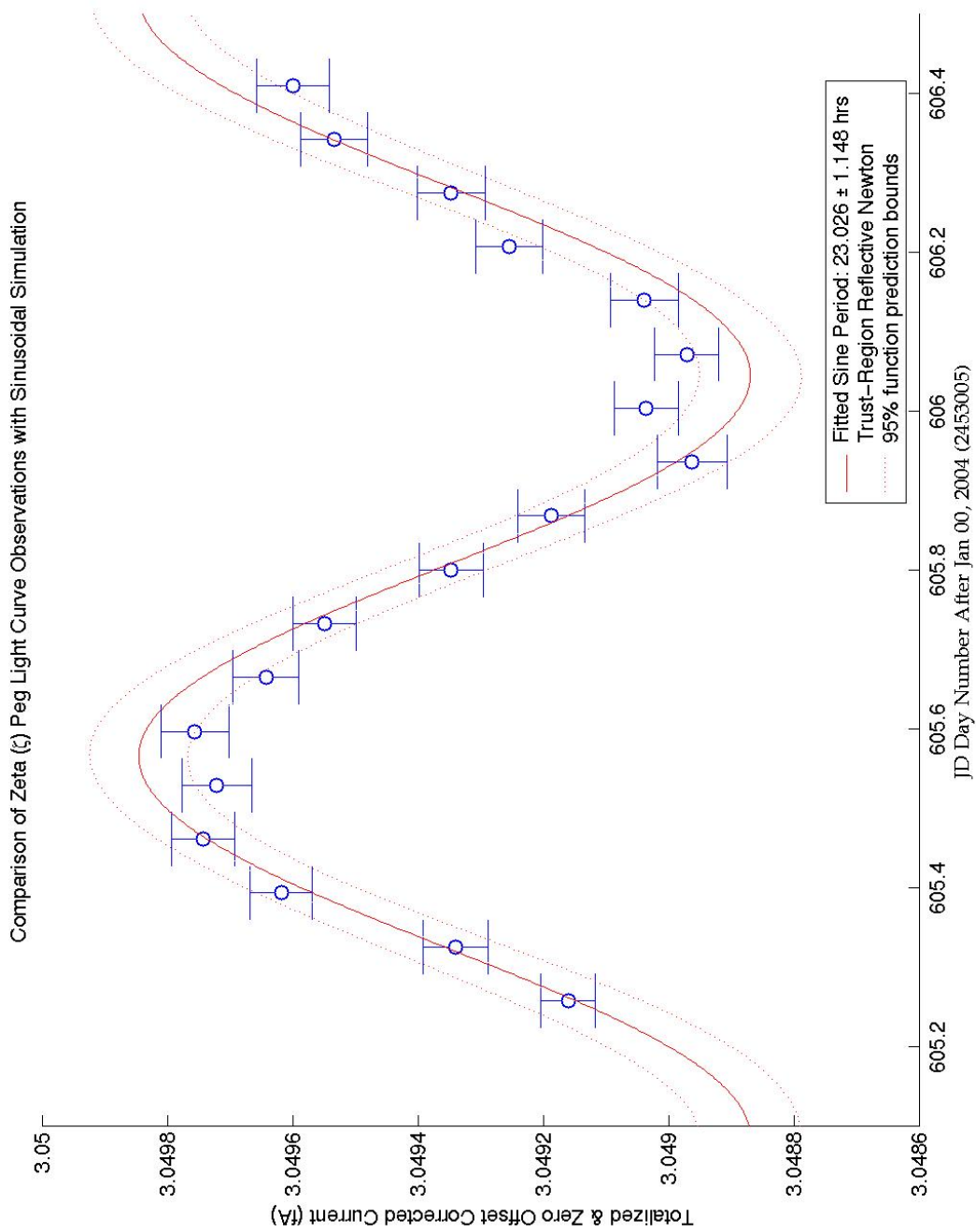
Figure 7. Comparison of the derived model with the observations of ζPeg. The dotted lines form the 95% confidence bounds.
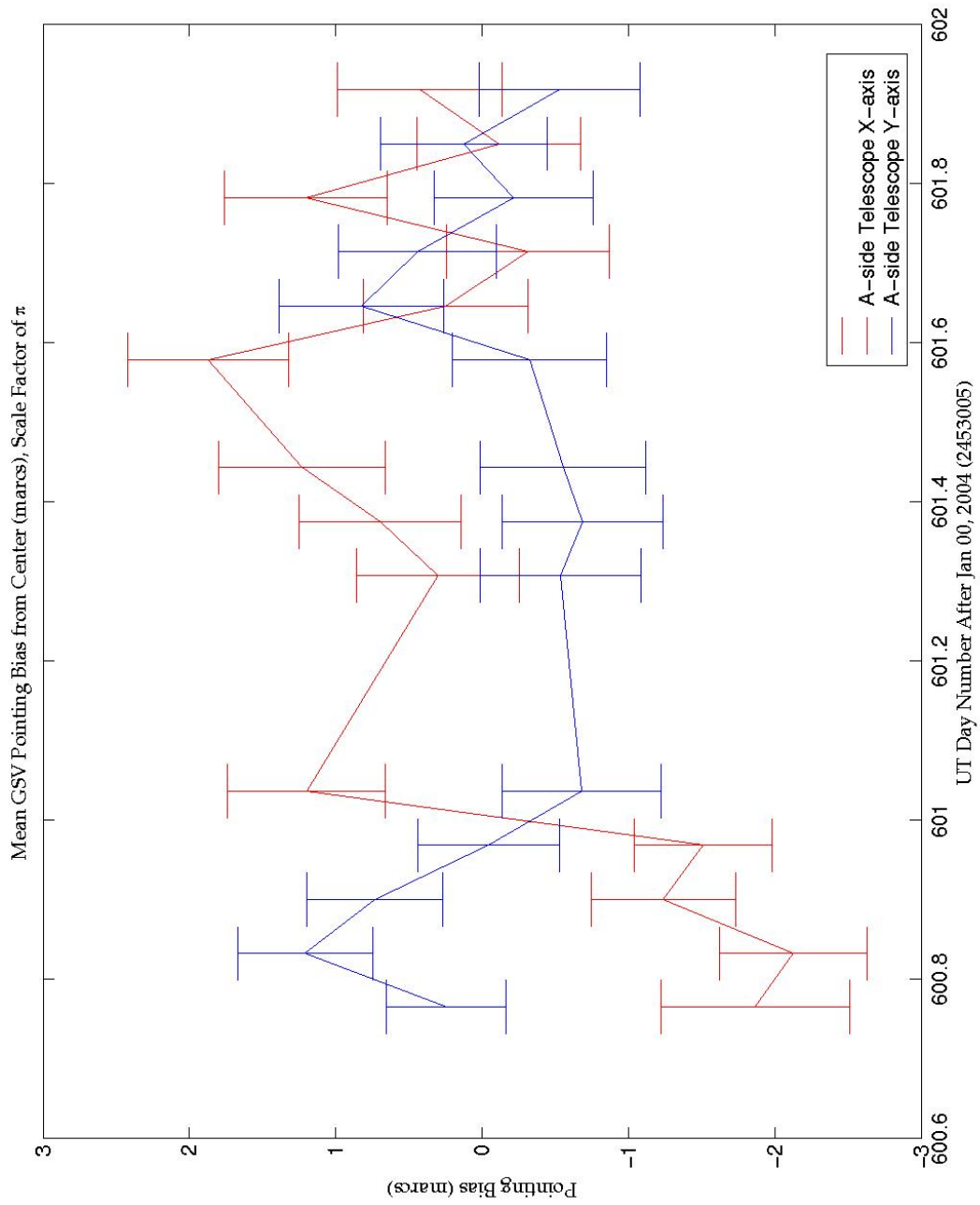
Figure 8. Pointing bias from center during observations of ζ Peg. One set of data is for the x-axis and the other is for the y-axis of the primary set of detectors. Each datum is for an entire orbit, or observation.
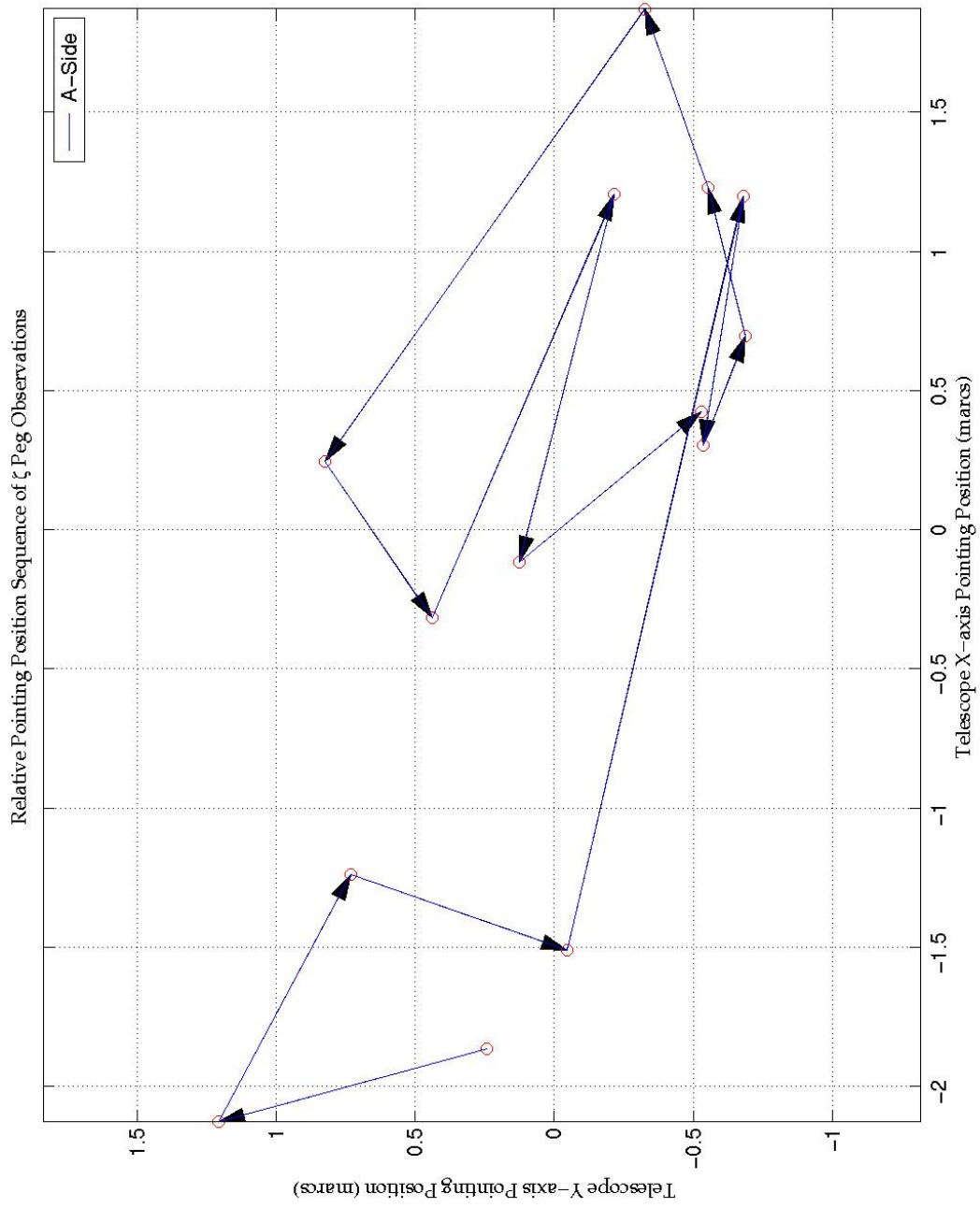
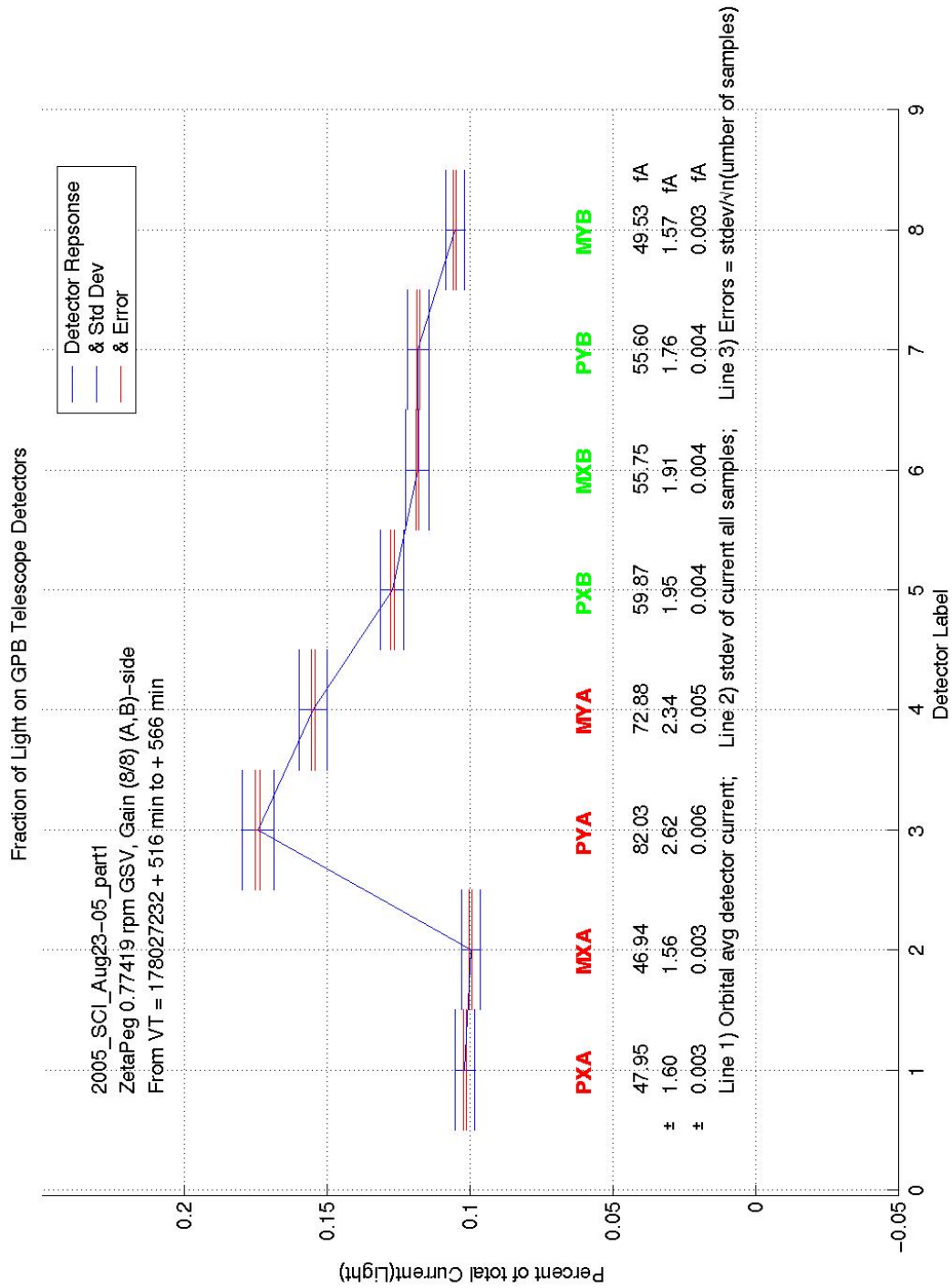Figure 9. Relative pointing bias excursions during observations of ζ Peg. Each point is an observation, the temporal sequence being indicated by the arrows.

Figure 10. Distribution of light on all eight detectors during guiding operations. Nominally, the star is centered on the Knife-edge Image Divider Assembly (KEIDA). Inner error bars are for precision; outer ones are for 1σ.
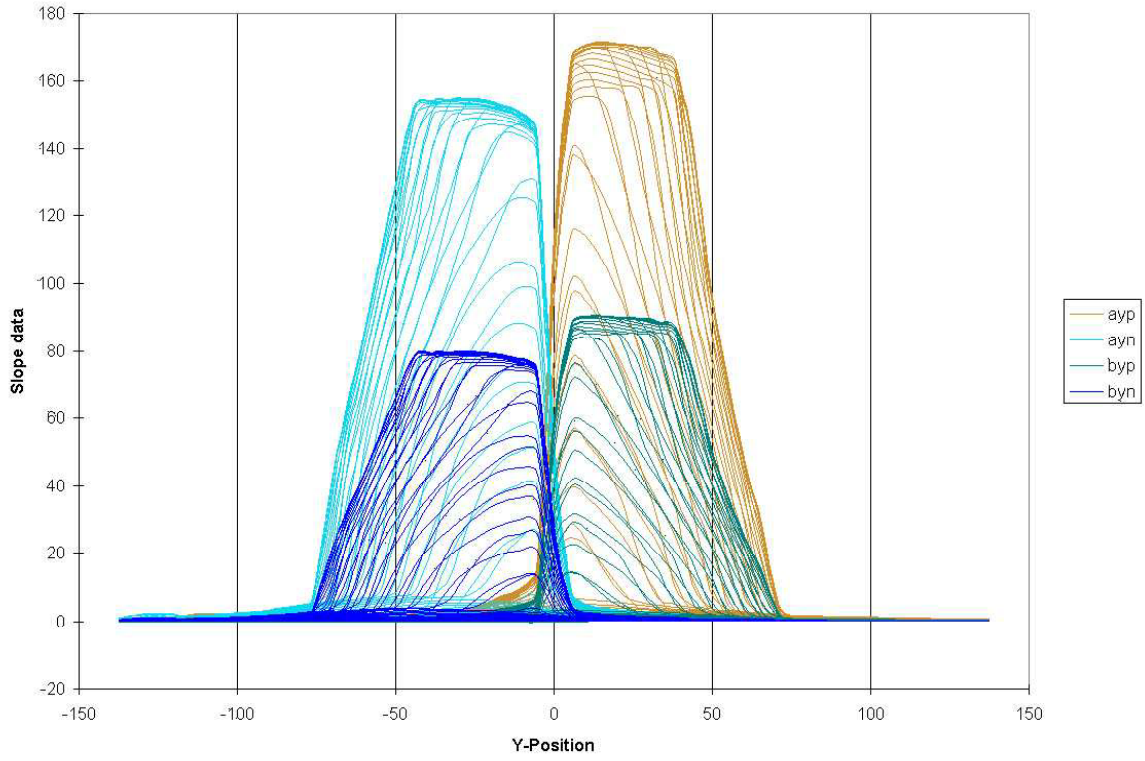
Figure 11. Y detector response scans from Artificial Star III and Telescope III data X raster of the AS III spot. Sets of lines for a given color result from stepping in the x-axis dimension.
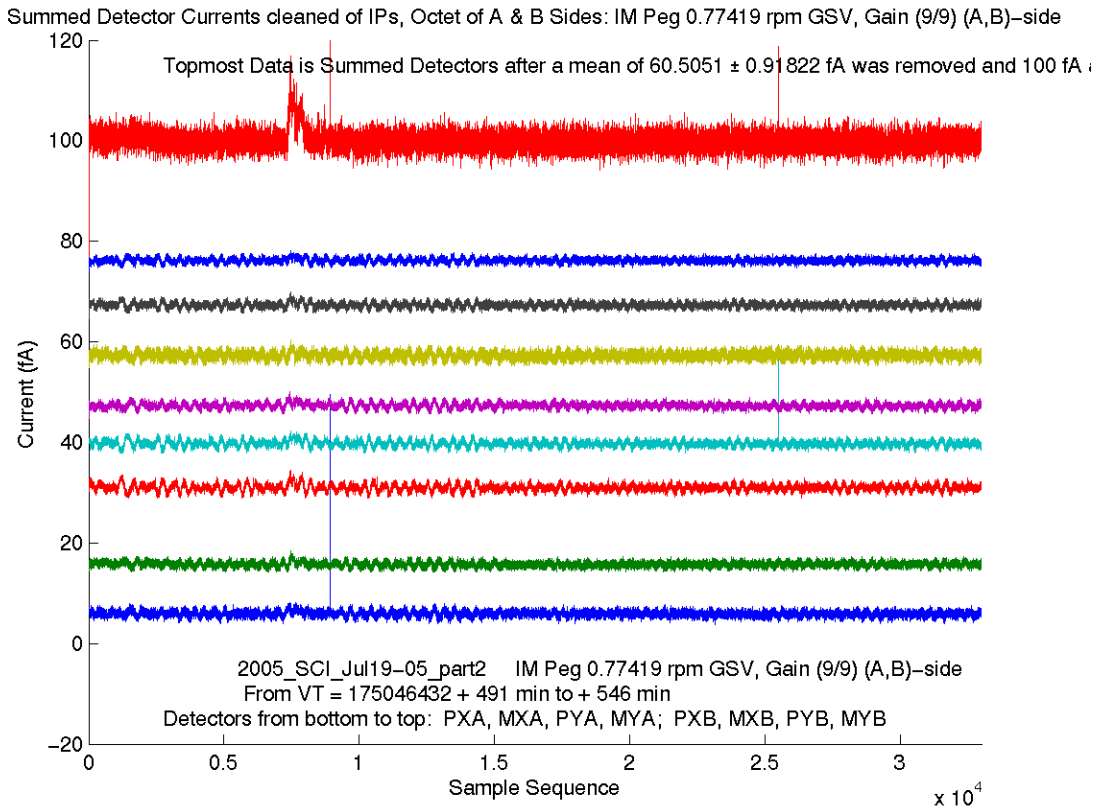
Figure 12. A display of individual detector responses during an orbital observation of IM Peg, the science phase guide star. An optical event occurred in all eight detectors simultaneously. It has been attributed to the maneuvering thruster exhaust of another satellite near the line of sight to IM Peg. Two uncensored proton events occurred.
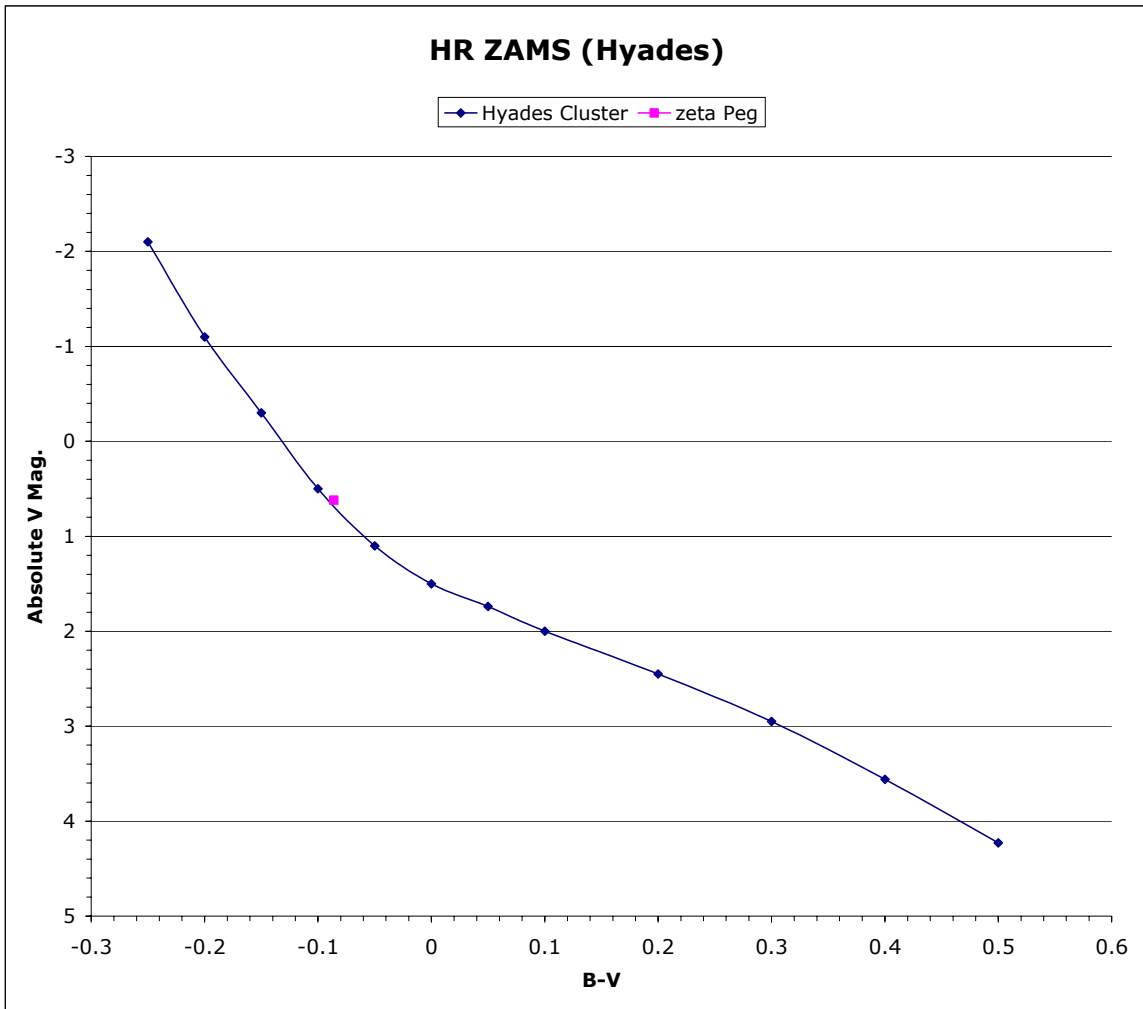
26

Figure 13. Location of ζ Peg in the Herzsprung-Russell (HR) diagram. The line is the location of the Zero Age Main Sequence (ZAMS) of stars in the Hyades cluster.
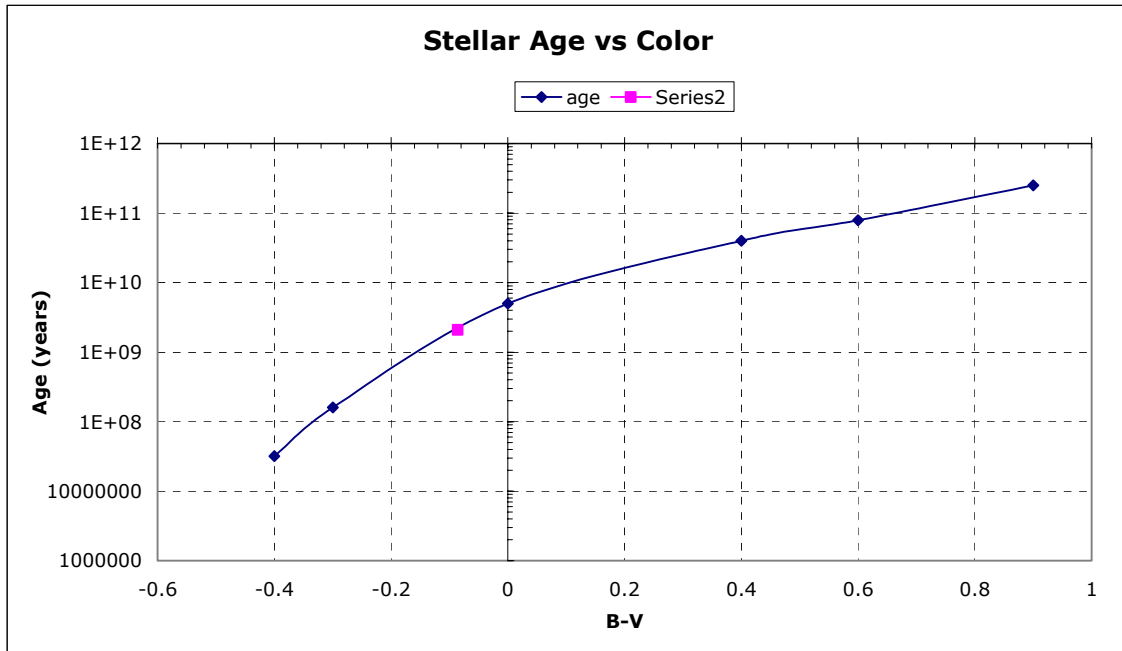
Figure 14. Stellar age in years versus color for the Hyades Cluster and ζ Peg (series2).
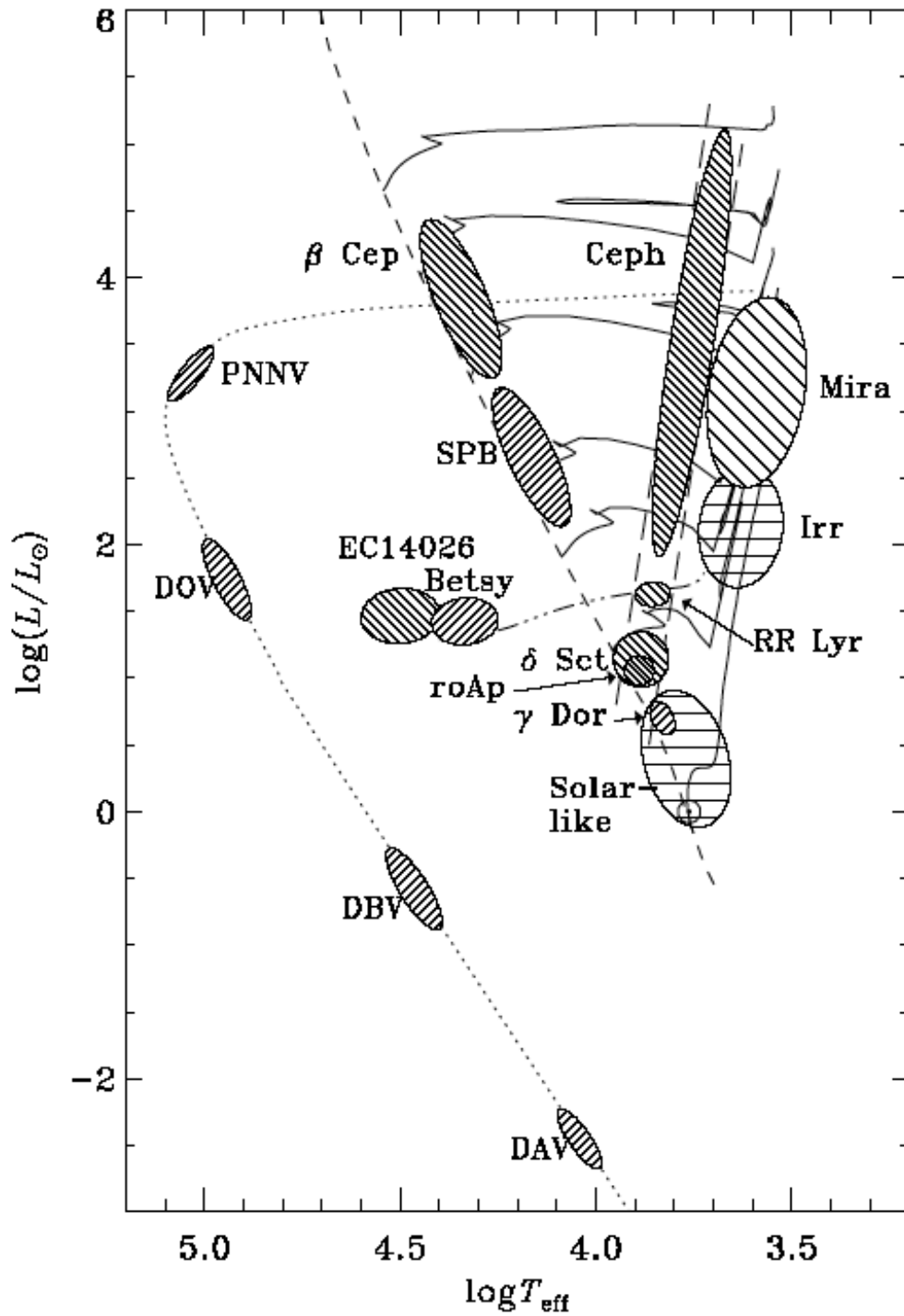
Figure 15. A pulsation HR Diagram showing many classes of pulsating stars for which asteroseismology is possible.

(From figure 11 of Kurtz (2006), reprinted by permission of Dr. J. Christensen-Dalsgaard.)
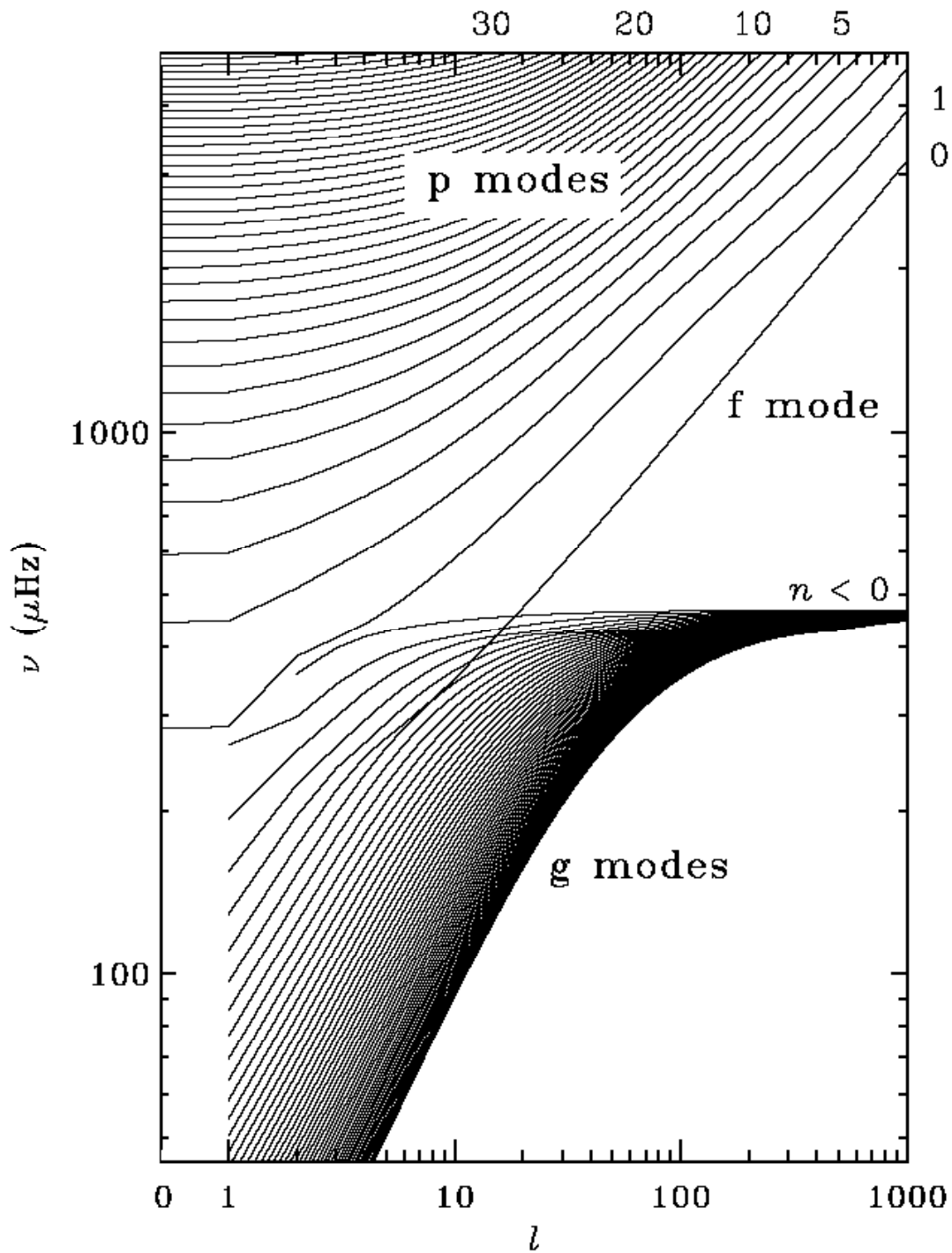
Figure 16. This diagram plots the degree l of a mode versus its frequency for a solar model.
(From figure 6 of Kurtz (2006), reprinted by permission of Dr. J. Christensen-Dalsgaard.)

Figure 17. Full spectral range of acoustic frequencies of ζ Peg and α Peg. The apparent emission peaks between 10 and 50 mHz are due to instrumental artifacts.

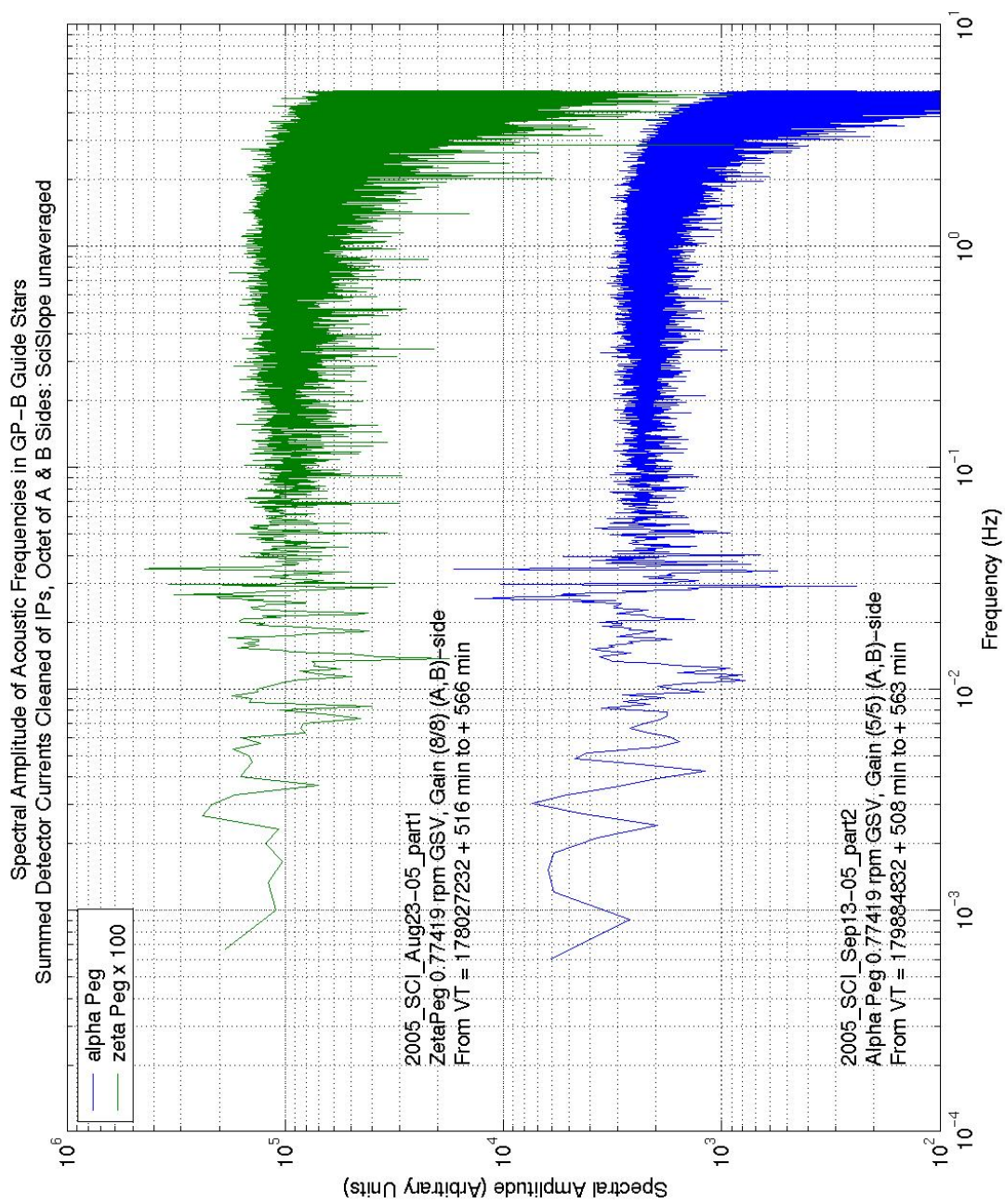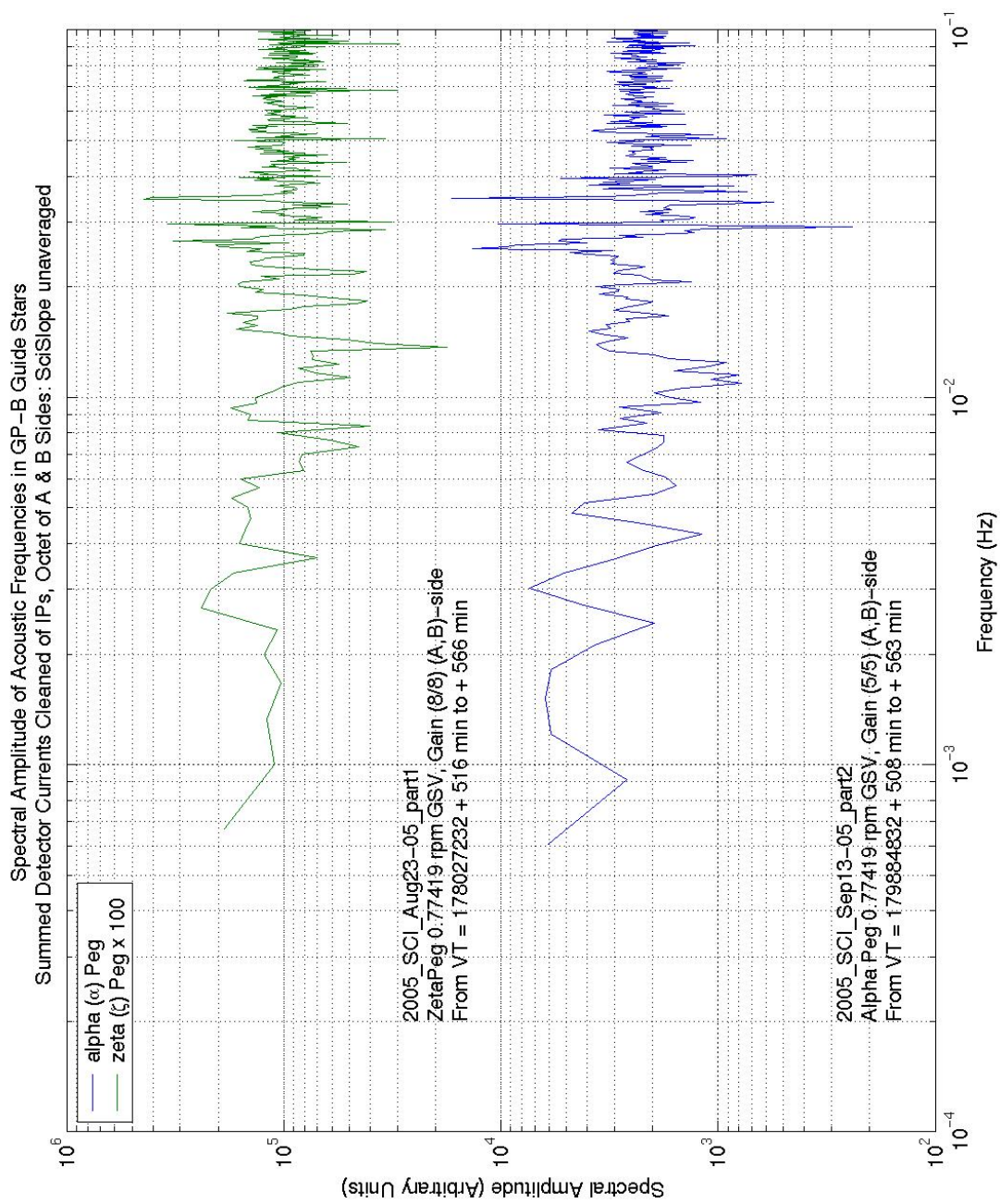Figure 18. Lowest spectral range of acoustic frequencies of ζ Peg and α Peg. The apparent emission peaks between 10 and 50 mHz are due to instrumental artifacts.

	REPORT DOCUMENTATION PAGE				Form Approved OMB No. 0704-0188

The public reporting burden for this collection of information is estimated to average 1 hour per response, including the time for reviewing instructions, searching existing data sources, gathering and maintaining the data needed, and completing and reviewing the collection of information. Send comments regarding this burden estimate or any other aspect of this collection of information, including suggestions for reducing this burden, to Department of Defense, Washington Headquarters Services, Directorate for information Operations and Reports (0704-0188), 1215 Jefferson Davis Highway, Suite 1204, Arlington, VA 22202-4302. Respondents should be aware that notwithstanding any other provision of law, no person shall be subject to any penalty for failing to comply with a collection of information if it does not display a currently valid OMB control number.
PLEASE DO NOT RETURN YOUR FORM TO THE ABOVE ADDRESS.

1. REPORT DATE *(DD-MM-YYYY)* 01/2007	2. REPORT TYPE Technical Publication	3. DATES COVERED *(From - To)*

4. TITLE AND SUBTITLE Zeta Pegasi: An SPB Variable Star	5a. CONTRACT NUMBER
	5b. GRANT NUMBER
	5c. PROGRAM ELEMENT NUMBER
6. AUTHOR(S) John H. Goebel	5d. PROJECT NUMBER
	5e. TASK NUMBER
	5f. WORK UNIT NUMBER 415113-04-01-01

7. PERFORMING ORGANIZATION NAME(S) AND ADDRESS(ES) Ames Research Center, Moffett Field, CA 94035-1000	8. PERFORMING ORGANIZATION REPORT NUMBER A-0600011

9. SPONSORING/MONITORING AGENCY NAME(S) AND ADDRESS(ES) National Aeronautics and Space Administration Washington, D.C. 20546-0001	10. SPONSORING/MONITOR'S ACRONYM(S) NASA
	11. SPONSORING/MONITORING REPORT NUMBER NASA/TP-2007-213492

12. DISTRIBUTION/AVAILABILITY STATEMENT
Unclassified — Unlimited   Distribution: Standard
Subject Category: 89
Availability: NASA/CASI (301) 621-0390

13. SUPPLEMENTARY NOTES   POC: John H. Goebel, Ames Research Center, MS 244-10, Moffett Field, CA 94035-1000 (650) 604-3188. Published as an internal document for the Gravity Probe-B Program at W.W. Hansen Experimental Physics Laboratory, Stanford University, Stanford, CA 94305-4085.

14. ABSTRACT

Broadband photometric observations of the bright star ζ Pegasi are presented that display brightness variability of 488.2 ±6.6 μmag (ppm) range with a period of 22.952 ±0.804 hr ($f \approx 1.04566$ c/d). The variation is mono-sinusoidal, so the star is recommended for membership in the class of small-amplitude Slowly Pulsating B-Stars (SPB) variables oscillating in a non-radial g-mode.

15. SUBJECT TERMS
Stars: individual, Zeta Pegasi (ζ Peg); NASA Mission: Gravity Probe-B (GP-B); Variable star (Slowly Pulsating B-Stars (SPB)); Photometry

16. SECURITY CLASSIFICATION OF:			17. LIMITATION OF ABSTRACT	18. NUMBER OF PAGES	19a. NAME OF RESPONSIBLE PERSON John H. Goebel
a. REPORT	b. ABSTRACT	c. THIS PAGE			
Unclassified	Unclassified	Unclassified	Unclassified	38	19b. TELEPHONE *(Include area code)* (650) 604-3188